

Jeffrey Ouyang-Zhang Jang Hyun Cho Xingyi Zhou Philipp Krähenbühl
The University of Texas at Austin

Abstract

Detection Transformer (DETR) directly transforms queries to unique objects by using one-to-one bipartite matching during training and enables end-to-end object detection. Recently, these models have surpassed traditional detectors on COCO with undeniable elegance. However, they differ from traditional detectors in multiple designs, including model architecture and training schedules, and thus the effectiveness of one-to-one matching is not fully understood. In this work, we conduct a strict comparison between the one-to-one Hungarian matching in DETRs and the one-to-many label assignments in traditional detectors with non-maximum supervision (NMS). Surprisingly, we observe one-to-many assignments with NMS consistently outperform standard one-to-one matching under the same setting, with a significant gain of up to 2.5 mAP. Our detector that trains Deformable-DETR with traditional IoU-based label assignment achieved 50.2 COCO mAP within 12 epochs (1× schedule) with ResNet50 backbone, outperforming all existing traditional or transformer-based detectors in this setting. On multiple datasets, schedules, and architectures, we consistently show bipartite matching is unnecessary for performant detection transformers. Furthermore, we attribute the success of detection transformers to their expressive transformer architecture. Code is available at <https://github.com/jozhang97/DETA>.

1. Introduction

Traditional object detectors [17, 27] treat detection as region (two-stage) or anchor (one-stage) classification. They assign the ground truth labels to one or many regions/anchors and produce a set of overlapping predictions for each object. They then remove duplicates via post-processing, namely non-maximal suppression (NMS). Recent transformer-based detectors [2] side-step explicit NMS, and learn a suppression strategy in training via a strict one-to-one bipartite matching loss. Over two years of exciting development, end-to-end detectors have shown significant progress [6–8, 14, 20, 22, 29, 33, 35, 40] and recently surpassed

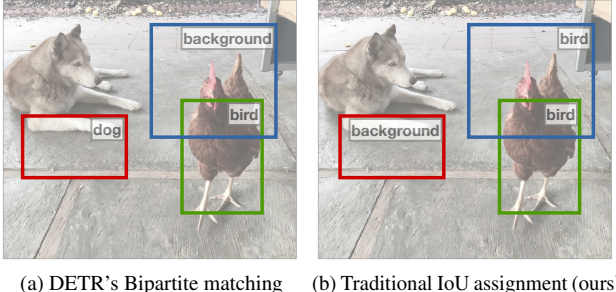


Figure 1. Detection Transformers vs. with traditional training objective. Presumable predicted boxes are visualized with ground truth object labels. (a) DETR-style bipartite matching matches one model prediction to one ground truth object such that the matched losses are minimized. (b) traditional IoU assignment assigns multiple anchors/proposals with high IoU to each ground truth object. Multiple positive labels enrich the training signal.

the performance of best traditional detectors [36]. However, detection transformers differ from traditional detectors along various axes: end-to-end design with Hungarian matching, heavier architectures (12 attention layers vs. 2 linear layers), longer training schedules (50 – 500 epochs vs. 12 epochs), etc. This makes it challenging to pinpoint what exactly contributes to good overall performance.

In this paper, we correct a widely-believed misconception that one-to-one mapping is essential for highly-performant detection. *Rather, the traditional one-to-many training objective yields equally proficient detection transformers.* We design a transformer-based object detector that directly *assigns* positive-negative labels to each query as in traditional detectors [17, 27] and use NMS to remove duplicated predictions, instead of using end-to-end one-to-one *matching*. We name our detector **DETA** (**D**etection **T**ransformers **A**ssignment).¹ Specifically, we follow the strong two-stage DETR framework [40], and replace the one-to-one Hungarian matching loss with a one-to-many IoU-based assignment loss in both stages. In the first stage, we assign anchors from

¹Here we highlight the distinction between “matching” and “assignment”: “matching” is from a dynamic algorithm, e.g., Hungarian matching; “assignment” is from a fixed rule, e.g., IoU-based assignment.

a transformer encoder to annotations or background using an IoU metric. In the second stage, we assign queries similarly. Our detector produces overlapping objects and uses NMS for post-processing. *DETA* has precisely the same architecture as its end-to-end counterparts.

Our hybrid architecture allows us to conduct strict comparisons with end-to-end transformer detectors and traditional detectors. Compared to traditional detectors [17, 27], *DETA* features a more expressive head: In the first stage, *DETA* uses a 6-layer transformer encoder over the convolutional backbone, while a traditional RPN [27] or RetinaNet [17] uses 2 to 4 convolutional layers; in the second-stage, *DETA* uses a 6-layer transformer decoder, while a traditional FasterRCNN [27] uses 2 linear layers. Compared to end-to-end transformer detectors [2, 40], *DETA* only differs in training loss, with exactly the same architecture. The effectiveness of our training loss comes from two properties. First, one-to-many mapping yields more total positive predictions which help speed up model convergence. Second, we use an object balancing technique that helps stabilize matching for small objects, which are shown to be especially challenging in end-to-end detectors [2]. We verify the advantages of both properties in our controlled experiments.

Our resulting detector is effective and easy to train. We show switching from standard bipartite matching to our IoU assignments in Deformable DETR [40] brings a significant 2.5 mAP improvement. Our model converges much faster than the existing transformer-based detector with superior performance, with 50.2 mAP on COCO under the standard $1 \times$ schedule (12 epochs) and ResNet50 backbone. This is 7.3 points higher than the best NMS-based detector (42.9 mAP of CenterNet2 [38]) and 0.8 points better than a strong end-to-end detector (49.4 mAP of DINO [36]). Our observation is consistent across different detection transformer architectures (DETR [2] and Deformable DETR [40]) and datasets (COCO [18] and LVIS [11]). On longer schedules and larger backbones, our traditional training objective can still replace bipartite objectives.

2. Related Work

Traditional NMS-based detectors map the input image to a downsampled dense feature map. Each pixel in the feature map is classified into an object class or background, resulting in overlapping predictions for each object. RetinaNet [17] and YOLO [24–26] define object or background by predefined IoU thresholds. CenterNet [39], FCOS [31], ATSS [37], and GFL [16] improve the IoU-based positive-negative definition to adaptive criteria. While multiple positive selection strategies [5, 37] are compatible with our method, we utilize the most common and straightforward fixed IoU threshold. Optionally, NMS-based detectors can be improved by a second stage [1, 3, 12, 27, 38], where the region features are refined using the IoU thresholds. Again, the second stage

outputs are duplicated and need NMS for post-processing.

Our work uses the simple IoU-based criterion from traditional detectors but also a transformer architecture.

End-to-end detectors. DETR [2] removes the duplication in detectors' predictions by directly mapping queries to unique objects using self-attention. The vanilla DETR is hard to train and has been improved by multiple follow-up works. Deformable-DETR [40] introduces multi-scale features with a deformable operation. Deformable-DETR, TSP-RCNN [29], and EfficientDETR [35] identify the learned object query as a causal factor for slow-convergence and replace them with a first-stage detector. Conditional-DETR [22] and DAB-DETR [20] concretize the implicit query as explicit point locations or boxes. DN-DETR [14] eases the one-to-one matching task by adding an auxiliary query de-noise loss. DINO [36] combines 2-stage queries and learned queries, and finally surpasses the performance of any existing NMS-based detectors.

All these works bring partial wisdom from NMS-based detectors but keep the Hungarian matching losses untouched. Our work is complementary to these ideas - we show a simple change in matching provides significant improvements.

GroupDETR [4] and \mathcal{H} -DETR [13] concurrently identified one-to-one matching as a training bottleneck. They train with additional queries in the transformer decoder to increase the number of matched queries and observe faster convergence and better performance. This validates our insight that more positive samples help. FQDet [23] finds that techniques from traditional detectors, such as IoU assignment and multiple anchor ratios, improve the convergence of detection transformers, however, they did not show significant performance improvements over detection transformers as ours. Our detector does not modify the architecture except for adding NMS and only modifies the training loss. We compare with these approaches in Sections 5.3 and 5.4.

3. Preliminary

Given an image $I \in \mathbb{R}^{H \times W \times 3}$, a detector produces a bounding box $b_i \in \mathbb{R}^4$ and scores $s_i \in \mathbb{R}^C$ for C categories for each object i .

DETR [2] decomposes detection into three components: a backbone, a transformer encoder, and a transformer decoder. The backbone takes the image as an input and produces a down-sampled D -dimensional feature map $F \in \mathbb{R}^{M \times D}$. Here M refers to the number of features in the feature map, $M = w \times h$ in vanilla DETR [2] or $M = \sum_l w_l \times h_l$ in multi-scale feature resolutions [40]. The *transformer encoder* refines F using self-attention with positional embeddings and produces updated features $F' \in \mathbb{R}^{M \times D'}$. The *transformer decoder* transform a set of queries $Q \in \mathbb{R}^{N \times D'}$ into N unique object detections (or background) $O = \{\hat{b}_i, \hat{s}_i\}_{i=1}^N$. During this process each query cross-attends to the encoded

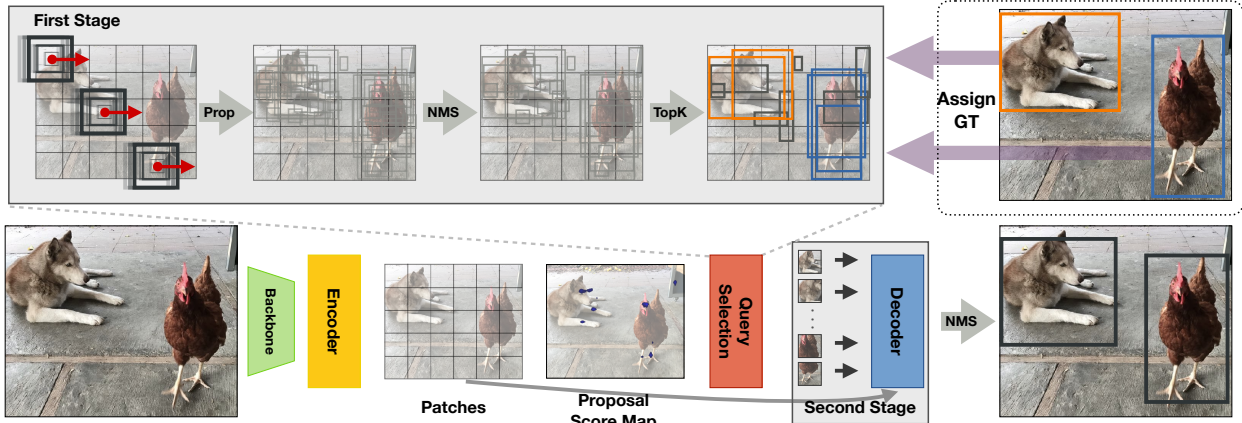


Figure 2. **Overview of our detection framework.** The transformer encoder extracts image features and a proposal score map (Bottom left). We sample top-ranking boxes as queries (Top left) and decode them with the image features. Each query reads out classification logits and a bounding box. The dotted section (Top right) shows our assignment procedure for the second stage during training. The orange and blue boxes indicate assigned proposals and objects.

feature map F' . Self-attention layers ensure objects O have little to no duplicates, and thus can learn non-maximum-suppression implicitly.

Two-stage DETR. In the vanilla DETR [2], the object queries Q are learnable network parameters and are fixed for all testing images. Multiple works [29, 35, 36, 40] show image-dependent queries improve convergence and performance. In the two-stage Deformable-DETR [40], the transformer encoder densely predicts ranked proposal boxes b_i^{prop} from fixed initial boxes b_i^{init} . The top N proposals form queries for a second stage $Q_i = \mathcal{G}(b_i^{\text{prop}})$. The second stage now takes features from the first stage as inputs instead of fixed queries. We follow this two-stage query formulation.

Hungarian matching loss. During training, DETR assigns each network output $O = \{\hat{b}_j, \hat{s}_j\}_{j=1}^M$ to exactly one annotated object in $G = \{b_k, c_k\}_{k=1}^K$ or background \emptyset where c_k is the class id for object k . Let $\sigma_i \in \{\emptyset, 1 \dots K\}$ be the assignment of network output i to annotation σ_i . DETR enforces a one-to-one matching to learn non-maxima-suppression: For $i \neq j$ with $\sigma_i \neq \emptyset$ and $\sigma_j \neq \emptyset$, we have $\sigma_i \neq \sigma_j$. Furthermore for each annotation k , $\exists i : \sigma_i = k$. DETR optimizes for the best matching in the training objective:

$$\mathcal{L}(O, G) = \min_{\sigma} \left(\underbrace{\sum_{i=1}^M \mathcal{L}_{cls}(\hat{s}_i, c_{\sigma_i}) + \mathcal{L}_{box}(\hat{b}_i, b_{\sigma_i})}_{\mathcal{L}(O, G | \sigma)} \right) \quad (1)$$

where \mathcal{L}_{cls} is a focal-loss based classification loss, and \mathcal{L}_{box} is a bounding box loss composed of GIoU and L1 loss. Any unmatched output $\sigma_i = \emptyset$ predicts a background score s_\emptyset , and incurs no box loss $\mathcal{L}_{box}(\hat{b}_i, b_\emptyset) = 0$. DETR finds the

optimal matching σ using the Hungarian algorithm².

In the following section, we show we can replace the one-to-one matching with a simple overlap-based assignment strategy to significantly boost the performance and training speed of DETR.

4. IoU assignment in transformer detectors

DETA changes the assignment procedure in Equation (1). We closely follow the assignment strategies of traditional two-stage detectors [27]. First, we relax the one-to-one matching constraint and instead allow one-to-many assignments. We allow multiple outputs i and j to be assigned to the same ground truth $\sigma_i = \sigma_j$. Second, we switch to a *fixed* overlap-based assignment strategy instead of the loss-based matching in Equation (1).

First stage assignments. We start from the fixed initial query features F derived from the Deformable-DETR architecture. Each query i is anchored at a specific location (x_i, y_i) within the image. However, proposals do not have a natural width and height required for box overlap metrics. We use a constant box size $w_i = 0.1 \times 2^{-l_i} \times W$ and $h_i = 0.1 \times 2^{-l_i} \times H$, where $l_i \in \{0, \dots, 3\}$ is the feature resolution, W and H are the width and height of the image. This yields an initial box definition $b_i^{\text{init}} = (x_i - \frac{w_i}{2}, y_i - \frac{h_i}{2}, x_i + \frac{w_i}{2}, y_i + \frac{h_i}{2})$. We use these initial boxes for both positional embeddings and the overlap-based assignment process. We assign each prediction i to the highest overlapping ground truth object if the overlap is larger than a threshold τ .

At the beginning of training, a ground truth object sometimes does not have an overlapping prediction with a thresh-

²In practice, DETR uses a different cost to match and supervise training.

old τ . We find no difference whether we keep the object unmatched or assigned to the closest unmatched prediction. For mathematical convenience here, we assume the latter. Anchor i is closest to object k if the condition

$$C_{\max}^{\text{init}}(i, k) = \bigcap_{j \neq i} \mathbb{1}\{IoU(b_i^{\text{init}}, b_k) \geq IoU(b_j^{\text{init}}, b_k)\} \quad (2)$$

is met. Then, the assignment procedure is formally

$$\sigma_i^{\text{init}} = \begin{cases} \hat{k} = \operatorname{argmax}_k IoU(b_i^{\text{init}}, b_k), & \text{if } IoU(b_i^{\text{init}}, b_{\hat{k}}) \geq \tau \\ & \text{or } C_{\max}^{\text{init}}(i, \hat{k}) \\ \emptyset, & \text{otherwise} \end{cases} \quad (3)$$

We use a threshold $\tau = 0.7$ for the first stage. Since the first stage uses a single box width and height per query feature, the resulting overlap metric IoU is very similar to the centerness estimate in anchor-free detectors [31, 38, 39].

We train the first stage using a class-agnostic version of the DETR loss $\mathcal{L}(O, G|\sigma^{\text{init}})$ (1) on our fixed assignments σ^{init} (3). The classification loss \mathcal{L}_{cls} of the first stage is a binary focal loss indicating foreground vs background. The first stage assignment procedure and loss formulation naturally encourage (near-)duplicate outputs. We follow Ren *et al.* [27] and apply non-maxima-suppression on the proposal boxes b^{prop} . It reduces the computational burden and increases coverage of the first-stage proposals.

Second stage assignments. The assignment procedure in the second stage closely follows the first stage assignment procedure. However, instead of using a fixed set of initial boxes b^{init} , we use the outputs of the first stage b^{prop} to define an equivalent assignment σ_i^{prop} . We train this second stage using the same loss as DETR $\mathcal{L}(O, G|\sigma^{\text{prop}})$. Following Faster RCNN [27], we balance the foreground object ratio using a hyper-parameter γ . Specifically, when the number of positive queries is larger than $N \times \gamma$, we randomly sample $N \times \gamma$ positive queries from them. To encourage a larger number of positive queries we relax the overlap criterion for the second stage to $\tau = 0.6$. This simple relaxation of the overlap criterion already works well for most mid-sized and large objects. However, small objects are under-sampled.

Object Balancing. In contrast to the one-to-one mapping that always has one matched prediction for each ground truth object, our IoU assignment might assign a dramatically different number of predictions across ground truth objects. Larger objects are naturally more likely to contain many overlapping predictions than smaller objects. This imbalance hurts performance. We propose a simple object-balancing technique that samples at most n positive assignments for each ground truth. Let μ_k^n be the n -th highest IoU for annotation k and $\tau_k^n = \max(\tau, \mu_k^n)$ be our new dynamic threshold. We modify the assignment procedure in Equation (3):

$$\sigma_i^{\text{prop}} = \begin{cases} \hat{k} = \operatorname{argmax}_k IoU(b_i^{\text{prop}}, b_k), & \text{if } IoU(b_i^{\text{prop}}, b_{\hat{k}}) \geq \tau_k^n \\ & \text{or } C_{\max}^{\text{prop}}(i, \hat{k}) \\ \emptyset, & \text{otherwise} \end{cases} \quad (4)$$

We verify balancing objects benefits small object performance in Section 5.6.

5. Results

We evaluate our method on the COCO 2017 and LVIS benchmarks [11, 19]. COCO contains 118k training and 5k validation images over 80 object categories. LVIS is a long-tail detection dataset with 1203 object categories. We report bounding box mAP as the evaluation metric.

5.1. Implementation Details

Unless other specified, we build off two-stage Deformable-DETR [40]. We follow detectron2 [34] to set traditional detection hyperparameters. Specifically, we set the IoU threshold $\tau' = 0.7$ in the first stage and $\tau = 0.6$ in the second stage. The foreground ratio γ is 0.5, 0.25 in the first and second stages, respectively. We use an NMS threshold of 0.9, 0.7 in the first and second stage. Prior to NMS, we filter to 1000 boxes per feature level in the first stage and 10000 boxes in the second stage. We set the object-balancing parameter $K = 4$ (Section 4) as swept in Table 8.

Improved DETR and Deformable-DETR baselines. For our main results, we start with an improved two-stage Deformable-DETR [40] baseline following DINO [36] with 900 queries (or proposals), 5 feature scales, larger feed-forward dimension, box refinement, etc. We also report performance with vanilla DETR by replacing deformable attention with vanilla attention. Due to memory constraints in vanilla self-attention, DETR uses features F from the last stage of the backbone with extra dilation and reduced stride (typically known as DC-5). The number of proposals becomes much smaller - for a 480×480 image, $M = 900$ for DETR’s DC-5 features whereas $M \approx 4800$ for Deformable-DETR’s multi-scale features. Since the number of proposals is close to the number of queries, we use 300 queries and keep bipartite matching in the first stage of DETR and only use IoU assignment in the second stage.

For ResNet-50 system-level comparisons, we additionally use 9 transformer encoder layers and evaluate with 300 predictions. In our ablations, we use the default Deformable-DETR [40] setting with 300 queries, 4 feature scales, 6 transformer encoder and decoder layers. All other training hyper-parameters strictly follow Deformable-DETR [40], i.e., we use ResNet50 backbone with AdamW optimizer with learning rate 0.002, and batch size 16. We train with a $1 \times$ schedule, with 90K iteration and learning rate dropped

#		COCO								LVIS			
		Deformable-DETR [40]				DETR [2]				Deformable-DETR [40]			
		AP	AP _s	AP _m	AP _l	AP	AP _s	AP _m	AP _l	AP	AP _s	AP _m	AP _l
1	Baseline	43.2	25.9	46.6	57.6	35.3	15.2	37.5	53.6	-	-	-	-
2	Improved baseline	47.7	31.2	51.0	61.8	41.8	22.3	44.6	59.7	31.5	22.1	41.2	48.3
3	+ IoU Asgmt & NMS w/o Object balance	48.7	30.9	53.1	64.4	41.8	21.3	46.2	61.2	31.5	21.5	41.0	50.0
4	+ Object balance (Ours)	50.2	32.2	54.4	64.6	43.9	24.6	48.2	60.8	33.9	23.2	44.0	52.7

Table 1. **IoU assignments vs. Hungarian matching.** We report AP on COCO ($1\times$ schedule for *Deformable-DETR*, 50 epoch for DETR) and LVIS (180k iter) validation with ResNet50 backbone. Row 1: the original baselines; Row 2: our improved baseline; Row 3: changing Hungarian matching in Row 2 to naive IoU assignment and re-introducing NMS; Row 4: applying our object balancing technique (Section 4) to Row 3. IoU assignment with object balancing significantly outperforms Hungarian matching. See Table 3 for longer schedules on COCO.

Module	DETA	Deformable-DETR
Backbone	22	22
Transformer Encoder	56	56
Query Selection	13	9
Transformer Decoder	8	8
Postprocess (NMS)	1	0
Total	100	95

Table 2. **Runtime breakdown in milliseconds.** Models use the ResNet-50 backbone. The module names are taken from Figure 2. NMS in query selection and postprocessing takes 5ms.

at the 75K iteration. Training takes ~ 18 hours on 8 Quadro RTX 6000.

5.2. Main results

We compare Hungarian matching from the original DETR [2] with our IoU assignments under multiple datasets and architectures in Table 1. We evaluate with Deformable DETR architecture on COCO under the $1\times$ schedule, DETR architecture on COCO under the 50 epoch schedule and LVIS under 180k iterations.

We first report the results of the original 2-stage Deformable DETR [40] alongside our improved baselines as described in Section 5.1. From the improved baseline, simply replacing the Hungarian matching with the naive traditional IoU assignments (without the object balance technique in Section 4) with NMS improves by 1.0 mAP on COCO. The improvements come with no additional cost except for NMS, which runs in a few milliseconds. This shows traditional overlapping assignments can likewise train transformers.

However, with assignment alone, there is no change in LVIS AP and DETR’s COCO AP. On LVIS, traditional assignment underperforms on small object AP (21.5 vs 22.1) while outperforming on large object AP (50.0 vs 48.3). We also see this trend in DETR where small object AP drops from 22.3 to 21.3 and large object AP increases from 59.7

to 61.2 on COCO. We hypothesize traditional assignments cause an imbalance in the number of positives per object as the larger objects have many more matches (and appear less frequently in LVIS [11]). Further balancing the number of matched ground truth brings an additional gain on all settings. On LVIS, object balancing increases AP by 2.4 points. On COCO, object balancing improves performance by 1.5, 2.1 mAP for Deformable DETR and vanilla DETR respectively. The improvements are more pronounced for small objects on COCO, with a delta of 1.3 mAP vs. 0.1 mAP in large objects for Deformable DETR.

5.3. Comparisons to prior works

Table 3 compares *DETA* to traditional NMS-based detectors and transformer-based end-to-end detectors on the COCO 2017 validation set with ResNet50 backbone. Traditional NMS-based detectors are usually efficient to train and converge with a short training schedule (12 epochs). Transformer-based end-to-end detectors require longer training schedules, i.e., from 36 to 500 epochs, and can achieve higher overall performance.

On the standard $1\times$ schedule, our model achieves the highest performance of 50.5 mAP, outperforming the next best method by 0.7 mAP. On the longer $2\times$ schedule, our model sees a 0.3 mAP performance gain. This suggests that traditional training assignments are competitive with bipartite-like matching in detection transformers and may even converge faster. At inference, our model runs at a comparable speed to Deformable-DETR [40]. Specifically, it runs 5% slower due to NMS taking 5 milliseconds. A detailed runtime breakdown between Deformable-DETR and *DETA* is shown in Table 2. *DINO* is slower partially because it uses larger feature resolutions, starting at $\frac{H}{4} \times \frac{W}{4}$.

5.4. Comparisons on large backbones

Table 4 compares our models to other detectors on larger backbones on COCO test-dev. We train *DETA* with Swin-L backbone for $2\times$ schedule on COCO with no additional data and obtain 58.5 mAP. With the exception of backbone

Method	Epochs	<i>AP</i>	<i>AP₅₀</i>	<i>AP₇₅</i>	<i>AP_S</i>	<i>AP_M</i>	<i>AP_L</i>	Params	FPS
Faster RCNN [27]	12	37.9	58.8	41.0	22.4	41.1	49.1	42M	17
FCOS [31]	12	38.6	57.4	41.4	22.3	42.5	49.8	32M	46
ATSS [37]	12	39.3	57.5	42.8	24.3	43.3	51.3	32M	-
GFL [15]	12	41.1	58.8	44.9	23.5	44.9	53.3	32M	19
Cascade RCNN [1]	12	42.1	59.8	45.8	24.3	45.2	54.8	72M	7
DyHead [7]	12	42.6	60.1	46.4	26.1	46.8	56.0	39M	-
CenterNet2 [38]	12	42.9	59.5	47.0	24.1	47.0	56.2	72M	18
HTC [3]	20	43.2	59.4	40.7	20.3	40.9	52.3	80M	3
DETR [2]	500	43.3	63.1	45.9	22.5	47.3	61.1	41M	37
Anchor DETR [33]	50	44.2	64.7	47.5	24.7	48.2	60.6	39M	17
TSP-RCNN+ [29]	96	45.0	64.5	49.6	29.7	47.7	58.0	-	15
Conditional DETR [22]	108	45.1	65.4	48.5	25.3	49.0	62.2	44M	34
Efficient DETR [35]	36	45.1	63.1	49.1	28.3	48.4	59.0	-	-
Deformable-DETR [40]	50	46.2	65.2	50.0	28.8	49.2	61.7	40M	18
FQDet [23]	24	46.2	65.3	49.2	29.1	50.3	61.0	42M	-
DAB-Deformable-DETR [20]	50	46.9	66.0	50.8	30.1	50.4	62.5	47M	15
Dynamic DETR [7]	36	47.2	-	-	-	-	-	58M	-
DN-Deformable-DETR [14]	50	48.6	67.4	52.7	31.0	52.0	63.7	48M	6
Group-DETR [4]	12	49.8	-	-	32.4	53.0	64.2	-	-
\mathcal{H} -Deformable-DETR [13]	36	50.0	68.3	54.4	32.9	52.7	65.3	48M	12
DINO [†] [36] (1× schedule)	12	49.4	66.9	53.8	32.3	52.5	63.9	47M	5
DINO [†] [36] (2× schedule)	24	51.3	69.1	56.0	34.5	54.2	65.8	47M	5
Improved Deformable-DETR [40]	12	47.7	65.9	52.0	31.2	51.0	61.8	48M	13
Improved Deformable-DETR [40]	50	49.6	67.8	54.2	32.5	52.7	63.9	48M	13
Improved Deformable-DETR* [40]	50	47.7	66.0	51.9	29.9	51.0	62.7	52M	11
Improved Deformable-DETR [†] [40]	50	49.8	68.3	54.4	33.2	52.9	64.0	48M	13
<i>DETA</i> (Ours 1× schedule) ^{*†}	12	50.5	67.6	55.3	33.1	54.7	65.2	52M	10
<i>DETA</i> (Ours 2× schedule)	24	51.1	68.5	56.4	34.3	55.4	65.4	48M	13
<i>DETA</i> (Ours 2× schedule) ^{*†}	24	51.6	69.0	56.7	34.0	55.8	66.5	52M	10

Table 3. **System-level Comparisons to prior work on COCO validation with ResNet50 backbone.** For each detector, we list the number of training epochs, detection accuracy, number of model parameters and frames-per-second (FPS). FPS was measured on the same V100 machine whenever possible. Italic FPS were copied from the original publication. Top block: traditional NMS-based detectors; Middle block: transformer-based end-to-end object detectors. Bottom block: our transformer-based and NMS-based detector. *DETA* enjoys the best of both worlds. It trains as fast as NMS-based detectors and achieves performance competitive with transformer-based detectors. Methods with [†] are evaluated with the top 300 predictions. Methods with * use 9 encoder layers.

and training on 16 GPUs for 2× schedule, this setup is identical to our setup in Table 1. Our method outperforms our Deformable-DETR baseline by 1.9mAP and performs comparably to the latest end-to-end detection transformers such as \mathcal{H} -Deformable-DETR [13] and DINO [36].

Additionally, we pre-train *DETA* on Object-365 [9] for 2× schedule and finetune on COCO with a lower learning rate and larger image sizes for 2× schedule. We evaluate with single-scale testing with no test-time augmentations. This achieves 63.5AP on the COCO test-dev set, compared to DINO’s 63.3AP. This verifies bipartite matching is not necessary on larger backbones.

5.5. Analysis

We analyze 3 key advantages of our IoU assignment over the one-to-one matching in the vanilla Deformable DETR.

Our decoder learns an easier function. Intuitively, classifying and refining the boundary of a region is an easier task than global recognition and deduplication. We quantify an “easier” task as one which trains well with lower model complexity and measure the performance drop when decreasing the number of transformer layers. Table 5 studies the model performance with fewer encoder or decoder layers.

The results show *DETA* is more robust to fewer encoder and decoder layers than *Deformable-DETR*. *Deformable-DETR* degrades severely with 3 and 1 encoder layer(s), drop-

Method	Backbone	Extra Data	<i>AP</i>	<i>AP₅₀</i>	<i>AP₇₅</i>	<i>AP_S</i>	<i>AP_M</i>	<i>AP_L</i>	FPS
Deformable-DETR [40]	ResNeXt-101-DCN	-	50.1	69.7	54.6	30.6	52.8	65.6	4.6
EfficientDet-D7x [30]	EfficientNet-D7x-BiFPN	-	55.1	73.4	59.9	-	-	-	6.5
ScaledYOLOv4 [32]	CSPDarkNet-P7	-	55.4	73.3	60.7	38.1	59.5	67.4	16
CenterNet2 [38]	Res2Net-101-DCN-BiFPN	-	56.4	74.0	61.6	38.7	59.7	68.6	5
CopyPaste [10]	EfficientNet-B7	Objects365	56.0	-	-	-	-	-	-
HTC++ [3, 21]	Swin-L	-	57.7	-	-	-	-	-	-
<i>H</i> -Deformable-DETR [13]	Swin-L	-	58.3	77.1	63.9	39.8	61.5	72.7	4.6
DINO [36]	Swin-L	-	58.6	76.9	64.1	39.4	61.6	73.2	2.7
Improved Deformable-DETR	Swin-L	-	56.6	75.6	61.9	38.8	60.4	73.5	4.3
<i>DETA</i> (Ours)	Swin-L	-	58.5	76.5	64.4	38.5	62.6	73.8	4.2
DINO [36]	Swin-L	Objects365	63.3	-	-	-	-	-	2.7
<i>DETA</i> (Ours)	Swin-L	Objects365	63.5	80.4	70.2	46.1	66.9	76.9	4.2

Table 4. **Comparisons to prior work with larger backbones on COCO test-dev.** The results are taken from original works except *H*-Deformable-DETR and DINO where models are taken from their repositories and evaluated on the official test server. We train our model with Swin-L backbone [21] with a $2\times$ schedule. FPS are reported on the same V100 machine whenever possible. Italicized FPS are taken from original texts. Top block: traditional NMS-based detectors; Middle block: transformer-based end-to-end object detectors. Bottom block: transformer-based detectors with Objects365 pretraining.

# Enc. layer	# Dec. layer	<i>DETA</i>	<i>Deformable-DETR</i>
6	6	46.5	43.2
6	3	46.3 (<i>-0.2</i>)	42.5 (<i>-0.7</i>)
	1	44.6 (<i>-1.9</i>)	28.9 (<i>-14.3</i>)
3	6	46.2 (<i>-0.3</i>)	41.2 (<i>-2.0</i>)
	3	43.3 (<i>-3.2</i>)	38.6 (<i>-4.6</i>)
	1	41.3 (<i>-5.2</i>)	24.1 (<i>-19.1</i>)
1	6	43.3 (<i>-3.2</i>)	38.4 (<i>-4.8</i>)
	3	40.3 (<i>-6.2</i>)	34.3 (<i>-4.1</i>)
	1	36.6 (<i>-9.9</i>)	18.2 (<i>-25.0</i>)

Table 5. **Number of transformer layers.** We experiment with ResNet50 and $1\times$ schedule without our improved baseline and object balancing technique. We report AP. The top row is the default setting. *Deformable-DETR* performance drops much more than *DETA* when using fewer layers. We verify **our decoder learns an easier function**.

ping by 2.0 and 4.8AP compared to 0.3AP and 3.2AP. Interestingly, *Deformable-DETR* degrades more significantly with fewer decoder layers. When we evaluate our standard 6 encoder layer model with a single decoder layer, performance drops by 1.9AP and 14.3 AP for *DETA* and *Deformable-DETR*. This supports that our model learns a simpler decoding process that can be expressed in fewer decoder layers. This simpler decoding will be beneficial for future lightweight detectors.

More positive samples help. Our IoU assignments inherently and implicitly assign one or more positive queries to each ground truth, while one-to-one matching guarantees

a single positive. We hypothesize more positive samples can speed up training and improve performance [14]. To verify this hypothesis, we design a **one-to-many** matching *Deformable-DETR* model that matches each ground truth to *exactly B* queries. This is typically referred to as B-matching and can be simply reduced to bipartite matching by duplicating the cost matrix B times. As this objective encourages overlapping predictions, we add NMS. Table 6 show the results of this *Deformable-DETR* variant. Surprisingly, we show this simple (and suboptimal) variant brings non-trivial improvements (+2.5 mAP under proper hyper-parameters). This suggests more positive samples are important in detection. Note that this matching scheme is balanced by design, with a fixed number of predictions (B) for each object.

***DETA* does not need self-attention in the decoder.** We study the role of self-attention and cross-attention in the transformer decoder in Table 7. We independently replace an attention mechanism with a feed-forward network to maintain parameter parity.

Replacing cross-attention is harmful to both *DETA* and *Deformable-DETR*. We postulate that heavy MLP processing of queries harms performance. Similar conclusions have been made about two-stage detectors, evident by their shallow region-of-interest heads.

Replacing self-attention is detrimental to *Deformable-DETR* only. *Deformable-DETR* outputs unique objects by optimizing a set objective. Thus, it is natural to require the self-attention set operation during decoding. Meanwhile, *DETA* can decode queries independently ³.

³An astute observer will notice queries can interact via cross attention. We clip deformable sampling to the boxes without performance drop.

First-stage	Second-stage	<i>AP</i>	<i>AP_S</i>	<i>AP_M</i>	<i>AP_L</i>
1	1	43.2	61.9	46.7	25.9
1	2	44.7	64.1	48.0	26.8
1	4	45.1	64.0	48.5	27.1
1	8	43.0	62.2	46.0	24.5
2	1	44.0	62.8	47.4	27.7
4	1	43.7	62.2	47.5	25.6
8	1	43.1	61.3	46.8	26.4
2	2	45.4	64.7	48.9	28.6
4	4	45.8	64.6	49.5	28.4

Table 6. **More positive matchings to *Deformable-DETR* help.** We experiment with ResNet50 and 1× schedule without our improved baseline. Top row: the default setting. Adding some positives to both the first and second stage helps.

Cross-attn	Self-attn	<i>DETA</i>	<i>Deformable-DETR</i>
✓	✓	46.5	43.2
✓		46.6	34.7
	✓	9.3	7.2

Table 7. **Analysis of attention layers in the transformer decoder.** We report AP on COCO validation with ResNet50 and 1× schedule without improved baseline or object balancing technique. The top row is the default setting. We replace all self-attention layers (2nd row) or cross-attention layers (3rd row) with MLPs for *DETA* and *Deformable-DETR*. Both detectors need cross-attention, but *DETA* does not need self-attention in the decoder.

5.6. Ablation on object balancing

An important design of *DETA* is to balance the number of predictions for each object during training. Table 8 varies K , the max number of predictions for each ground truth object. A small K will aggressively filter assigned predictions and may slow down training. A large K may ignore detrimental sampling biases. $K = \infty$ does not balance objects.

The performance sweet spot at $K = 4$ improves small, medium, large AP by 1.6, 1.3, 0.5 over no balancing. Notably, the gain comes from smaller object performance. This is likely caused by a sampling bias resulting in fewer small object queries. Surprisingly, we observe a performance gap between $K = 1$ and bipartite matching despite both methods matching ground truth objects once. $K = 1$ improves small, medium, large AP by 2.7, 1.3, 1.4 points, respectively. This indicates that the sampling mechanism in vanilla bipartite matching is suboptimal, especially on small objects.

6. Limitations

DETA re-introduces NMS postprocessing to remove over-

K	<i>AP</i>	<i>AP_S</i>	<i>AP_M</i>	<i>AP_L</i>
∞	46.5	28.4	50.2	63.0
16	47.0	27.6	50.8	63.2
8	47.6	29.2	51.3	63.8
4	47.9	30.0	51.5	63.5
1	46.1	28.6	49.4	60.3
Bipartite	43.2	25.9	46.6	57.6

Table 8. **Ablation on Object Balancing of *DETA* in Section 4.**

We report results on COCO validation with ResNet50 and 1× schedule without the improved baseline. K is the hyper-parameter for the maximum predictions of a ground truth object. $K = \infty$ (first row) means without object balancing. We sweep K in a log scale (middle block). We also compare to the default one-to-one bipartite in Deformable DETR in the bottom row. Object balancing improves AP by 1.4%, and is especially useful for small and medium objects.

lapping objects. The NMS thresholds can be task-specific and challenging to tune. For example, while NMS with a threshold of 0.5 is fine for COCO images, it struggles with CrowdHuman [28] images that contain objects in a crowd scene. *DETA* no longer specifies objects uniquely with queries. This may change how the model will leverage queries in downstream tasks. *DETA* assumes we have an initial bounding box representation to which we can assign an object. This is realized by the two-stage framework where the queries are initialized by a bounding box. One drawback is that the method can only work with queries that represent bounding boxes. However, most well-performing transformer-based detectors seem to use two-stage query formulation [36, 40].

7. Conclusions

Assignments effectively train detection transformers. Our proposed training with IoU-based label assignment is more efficient than vanilla one-to-one matching of detection transformers. We analyzed empirically that assignment-based training benefits from 1) learning easier decoding function, 2) learning from more positive samples, and 3) not needing to globally optimize via self-attention. From our analyses, we showcase an arguably simpler alternative training mechanism of detection transformer compared to recent detection transformer methods [14, 36]. This alternative enjoys a significant advantage in training efficiency, especially with a short training schedule. We deduce that the effectiveness of detection transformer comes from its transformer encoder and decoder architecture.

Acknowledgements This material is in part based upon work supported by the National Science Foundation under Grant No. IIS-1845485 and IIS-2006820.



Figure 3. **Example visualization of positive and negative matches on COCO validation.** We visualize images with ground truth boxes (top), *Deformable-DETR* predictions (middle), and our predictions (bottom). We use the oracle labels only to match each ground truth object. Our prediction color scheme is as follows. **Green:** prediction matched to a ground truth object. **Red:** high confidence (>0.3) prediction matched to background. We find that bipartite matching in *Deformable-DETR* does not match well-localized object predictions.

References

- [1] Zhaowei Cai and Nuno Vasconcelos. Cascade r-cnn: Delving into high quality object detection. In *CVPR*, 2018. [2, 6](#)
- [2] Nicolas Carion, Francisco Massa, Gabriel Synnaeve, Nicolas Usunier, Alexander Kirillov, and Sergey Zagoruyko. End-to-end object detection with transformers. In *ECCV*, 2020. [1, 2, 3, 5, 6](#)
- [3] Kai Chen, Jiangmiao Pang, Jiaqi Wang, Yu Xiong, Xiaoxiao Li, Shuyang Sun, Wansen Feng, Ziwei Liu, Jianping Shi, Wanli Ouyang, et al. Hybrid task cascade for instance segmentation. In *CVPR*, 2019. [2, 6, 7](#)
- [4] Qiang Chen, Xiaokang Chen, Gang Zeng, and Jingdong Wang. Group detr: Fast training convergence with decoupled one-to-many label assignment. *arXiv preprint arXiv:2207.13085*, 2022. [2, 6](#)
- [5] Qiang Chen, Yingming Wang, Tong Yang, Xiangyu Zhang, Jian Cheng, and Jian Sun. You only look one-level feature. In *Proceedings of the IEEE/CVF conference on computer vision and pattern recognition*, pages 13039–13048, 2021. [2](#)
- [6] Bowen Cheng, Alexander G. Schwing, and Alexander Kirillov. Per-Pixel Classification is Not All You Need for Semantic Segmentation. *NeurIPS*, 2021. [1](#)
- [7] Xiyang Dai, Yinpeng Chen, Bin Xiao, Dongdong Chen, Mengchen Liu, Lu Yuan, and Lei Zhang. Dynamic head: Unifying object detection heads with attentions. In *CVPR*, 2021. [1, 6](#)
- [8] Zhigang Dai, Bolun Cai, Yugeng Lin, and Junying Chen. Up-detr: Unsupervised pre-training for object detection with transformers. In *CVPR*, 2021. [1](#)
- [9] Yuan Gao, Hui Shen, Donghong Zhong, Jian Wang, Zeyu Liu, Ti Bai, Xiang Long, and Shilei Wen. A solution for densely annotated large scale object detection task. https://www.objects365.org/slides/Obj365_BaiduVIS.pdf, 2019. [6](#)
- [10] Golnaz Ghiasi, Yin Cui, Aravind Srinivas, Rui Qian, Tsung-Yi Lin, Ekin D Cubuk, Quoc V Le, and Barret Zoph. Simple copy-paste is a strong data augmentation method for instance segmentation. In *CVPR*, 2021. [7](#)
- [11] Agrim Gupta, Piotr Dollar, and Ross Girshick. LVIS: A dataset for large vocabulary instance segmentation. In *CVPR*, 2019. [2, 4, 5](#)
- [12] Kaiming He, Georgia Gkioxari, Piotr Dollár, and Ross Girshick. Mask r-cnn. In *ICCV*, 2017. [2](#)
- [13] Ding Jia, Yuhui Yuan, Haodi He, Xiaopei Wu, Haojun Yu, Weihong Lin, Lei Sun, Chao Zhang, and Han Hu. Detrs with hybrid matching. *arXiv preprint arXiv:2207.13080*, 2022. [2, 6, 7](#)
- [14] Feng Li, Hao Zhang, Shilong Liu, Jian Guo, Lionel M Ni, and Lei Zhang. DN-DETR: Accelerate DETR Training by

- Introducing Query DeNoising. *CVPR*, 2022. 1, 2, 6, 7, 8
- [15] Xiang Li, Wenhui Wang, Xiaolin Hu, Jun Li, Jinhui Tang, and Jian Yang. Generalized Focal Loss V2: Learning Reliable Localization Quality Estimation for Dense Object Detection. *CVPR*, 2021. 6
- [16] Xiang Li, Wenhui Wang, Lijun Wu, Shuo Chen, Xiaolin Hu, Jun Li, Jinhui Tang, and Jian Yang. Generalized Focal Loss: Learning Qualified and Distributed Bounding Boxes for Dense Object Detection. In *NeurIPS*, 2020. 2
- [17] Tsung-Yi Lin, Priya Goyal, Ross Girshick, Kaiming He, and Piotr Dollár. Focal loss for dense object detection. In *ICCV*, 2017. 1, 2
- [18] Tsung-Yi Lin, Michael Maire, Serge Belongie, James Hays, Pietro Perona, Deva Ramanan, Piotr Dollár, and C Lawrence Zitnick. Microsoft COCO: Common objects in context. In *ECCV*, 2014. 2
- [19] Tsung-Yi Lin, Michael Maire, Serge Belongie, James Hays, Pietro Perona, Deva Ramanan, Piotr Dollár, and C Lawrence Zitnick. Microsoft coco: Common objects in context. In *ECCV*, 2014. 4
- [20] Shilong Liu, Feng Li, Hao Zhang, Xiao Yang, Xianbiao Qi, Hang Su, Jun Zhu, and Lei Zhang. DAB-DETR: Dynamic anchor boxes are better queries for DETR. *ICLR*, 2022. 1, 2, 6
- [21] Ze Liu, Yutong Lin, Yue Cao, Han Hu, Yixuan Wei, Zheng Zhang, Stephen Lin, and Baining Guo. Swin transformer: Hierarchical vision transformer using shifted windows. *ICCV*, 2021. 7
- [22] Depu Meng, Xiaokang Chen, Zejia Fan, Gang Zeng, Houqiang Li, Yuhui Yuan, Lei Sun, and Jingdong Wang. Conditional DETR for Fast Training Convergence. *ICCV*, 2021. 1, 2, 6
- [23] Cédric Picron, Punarjay Chakravarty, and Tinne Tuytelaars. Fqdet: Fast-converging query-based detector. *arXiv preprint arXiv:2210.02318*, 2022. 2, 6
- [24] Joseph Redmon, Santosh Divvala, Ross Girshick, and Ali Farhadi. You only look once: Unified, real-time object detection. In *CVPR*, 2016. 2
- [25] Joseph Redmon and Ali Farhadi. YOLO9000: better, faster, stronger. In *CVPR*, 2017. 2
- [26] Joseph Redmon and Ali Farhadi. Yolov3: An incremental improvement. *arXiv preprint arXiv:1804.02767*, 2018. 2
- [27] Shaoqing Ren, Kaiming He, Ross Girshick, and Jian Sun. Faster R-CNN: Towards real-time object detection with region proposal networks. In *NIPS*, 2015. 1, 2, 3, 4, 6
- [28] Shuai Shao, Zijian Zhao, Boxun Li, Tete Xiao, Gang Yu, Xiangyu Zhang, and Jian Sun. Crowdhuman: A benchmark for detecting human in a crowd. *arXiv:1805.00123*, 2018. 8
- [29] Zhiqing Sun, Shengcao Cao, Yiming Yang, and Kris Kitani. Rethinking transformer-based set prediction for object detection. *ICCV*, 2021. 1, 2, 3, 6
- [30] Mingxing Tan, Ruoming Pang, and Quoc V Le. Efficientdet: Scalable and efficient object detection. In *CVPR*, 2020. 7
- [31] Zhi Tian, Chunhua Shen, Hao Chen, and Tong He. FCOS: Fully convolutional one-stage object detection. In *ICCV*, 2019. 2, 4, 6
- [32] Chien-Yao Wang, Alexey Bochkovskiy, and Hong-Yuan Mark Liao. Scaled-YOLOv4: Scaling Cross Stage Partial Network. *CVPR*, 2021. 7
- [33] Yingming Wang, Xiangyu Zhang, Tong Yang, and Jian Sun. Anchor detr: Query design for transformer-based detector. *arXiv preprint arXiv:2109.07107*, 2021. 1, 6
- [34] Yuxin Wu, Alexander Kirillov, Francisco Massa, Wan-Yen Lo, and Ross Girshick. Detectron2. <https://github.com/facebookresearch/detectron2>, 2019. 4
- [35] Zhuyu Yao, Jiangbo Ai, Boxun Li, and Chi Zhang. Efficient DETR: Improving End-to-End Object Detector with Dense Prior. *arXiv preprint arXiv:2104.01318*, 2021. 1, 2, 3, 6
- [36] Hao Zhang, Feng Li, Shilong Liu, Lei Zhang, Hang Su, Jun Zhu, Lionel M Ni, and Heung-Yeung Shum. Dino: Detr with improved denoising anchor boxes for end-to-end object detection. *arXiv preprint arXiv:2203.03605*, 2022. 1, 2, 3, 4, 6, 7, 8
- [37] Shifeng Zhang, Cheng Chi, Yongqiang Yao, Zhen Lei, and Stan Z Li. Bridging the gap between anchor-based and anchor-free detection via adaptive training sample selection. In *CVPR*, 2020. 2, 6
- [38] Xingyi Zhou, Vladlen Koltun, and Philipp Krähenbühl. Probabilistic two-stage detection. In *arXiv:2103.07461*, 2021. 2, 4, 6, 7
- [39] Xingyi Zhou, Dequan Wang, and Philipp Krähenbühl. Objects as Points. *arXiv:1904.07850*, 2019. 2, 4
- [40] Xizhou Zhu, Weijie Su, Lewei Lu, Bin Li, Xiaogang Wang, and Jifeng Dai. Deformable DETR: Deformable Transformers for End-to-End Object Detection. *ICLR*, 2021. 1, 2, 3, 4, 5, 6, 7, 8